Nitrogen recovery from pig slurry by struvite precipitation using a low-cost magnesium oxide

S. Astals[1*], M. Martínez-Martorell[1], S. Huete-Hernández[2], V.B. Aguilar-Pozo[1,2], J. Dosta[1], J.M. Chimenos[2]

[1] Department of Chemical Engineering and Analytical Chemistry, University of Barcelona, 08028 Barcelona, Spain.

[2] Department of Materials Science and Physical Chemistry, University of Barcelona, 08028 Barcelona, Spain.

* Corresponding author: sastals@ub.edu

Highlights

- Stabilizing agent (SA) made of MgO by-product and H3PO4 for struvite precipitation.
- The H3PO4/MgO ratio controls the mineral phase of the SA, bobierrite – newberyite.
- Newberyite-rich SA showed the highest TAN recovery efficiency from pig slurry.
- The most economical treatment cost was 7.5 € per kg of ammonia nitrogen recovered.
- Results were validated synthesising the optimum SA in a 200-L pilot plant.

ABSTRACT

Ammonia nitrogen management is a recurrent problem in intensive livestock areas. Struvite precipitation stands as a mature technology to recover ammonia nitrogen and prevent associated environmental problems. However, the feasibility of struvite technology to recover ammonia nitrogen from pig manure is limited by the reagents cost. This research aimed to optimise the formulation of a stabilizing agent (SA) synthesised using an industrial low-grade MgO by-product (LG-MgO) and phosphoric acid for efficient TAN recovery via struvite precipitation. Experimental results showed that the H_3PO_4/LG-MgO ratio controls the magnesium phosphate mineral phase of the SA (bobierrite and/or newberyite). Newberyite-rich SA showed the highest TAN removal efficiency from pig manure (66–73%) compared to the SA formed by a mixture of newberyite and bobierrite (51–59%) and by bobierrite (26%). Particle size reduction of LG-MgO did not improve the SA's TAN removal efficiency, although XRD patterns showed that the precipitates from the TAN removal experiments contained some unreacted newberyite. The economic analysis showed that the higher reactivity of the SA formulated using higher H_3PO_4/LG-MgO ratios compensated reagent costs. The SA synthesised with a H_3PO_4/LG-MgO ratio of 0.98 showed the most economical treatment cost, which was estimated at 7.5 € per kg of ammonia nitrogen from pig manure. Finally, the optimum SA was successfully synthesised in a 200-L pilot plant, with a TAN removal capacity only 10% lower than the one synthesised at lab-scale.

KEYWORDS

Nutrient recovery; Magnesium ammonium phosphate; Pig manure; Magnesium oxide; Magnesium by-products

1. INTRODUCTION

Traditional farming systems used crop residues for soil amendment and animal feed and the excrements from these animals as land fertiliser, which constituted a closed-loop relationship between soil fertility, crop residues and livestock (Bationo et al., 2007). However, higher market demands, the development of farming equipment, and the availability of cheaper livestock feed have led to intensive livestock farming (Giner Santonja et al., 2017). Worldwide, livestock production is concentrated in certain regions, where there is not enough land available to utilise all the manure as fertiliser (Kamilaris et al., 2020). If improperly managed, these may lead to the eutrophication of water bodies and an excessive increase in nitrate concentrations in drinking water sources. In this regard, the European Union Nitrate Directive (91/676/EEC) established a maximum dosage of 170 kg N/ha per year to protect water bodies against pollution caused by nitrates from agricultural sources (Musacchio et al., 2020).

Despite the European Union Nitrate Directive, groundwater contamination by nitrate is still a serious problem since about 20% of the monitoring stations in the European Union (EU) have an average concentration above 40 mg NO_3^--N/L (Report SWD(2018)246 final, 2108). Consequently, the European Commission has urged state countries to take further action in order to comply with the directive. Accordingly, in Catalonia (north-eastern Spain), the Catalan Government has issued a new decree regulating farms growth (Decret 153/2019). Briefly, the new decree bans the increase of livestock units for farms located in 66 municipalities for two years, while limiting the capacity to grow for farms located in over 400 municipalities unless the additional nitrogen load is removed/recovered through treatment or applied as fertiliser outside the designated vulnerable zones. The decree also fixed a minimum ratio for storage tanks (for

circular basins the height/diameter ratio ≥ 0.25) to minimise ammonia (NH_3) emissions during storage and the associated air pollution and ecosystem degradation (Sommer et al., 2017). Similarly, treatment technologies must remove or recover ammonia nitrogen rather than stripping it to the atmosphere.

Biological nitrification-denitrification stands as the most widespread technology to remove ammonia nitrogen from wastewater, including pig slurry (García-González et al., 2016; Siegrist, 1996; Türker and Çelen, 2007). However, nitrification-denitrification does not allow recovering the nitrogen contained in the wastewater and it is associated with N_2O emissions (Cruz et al., 2019; Ye et al., 2018). Additionally, biological systems display lower efficiencies when subjected to flow and composition fluctuations related to production cycles, start-up periods due to cease in production, and low temperatures. Due to these limitations, it is plausible to integrate biological systems with physico-chemical technologies (e.g. stripping, zeolite addition, clay addition and struvite precipitation) to guarantee the targeted nitrogen removal efficiency (De Vrieze et al., 2019). Accordingly, physico-chemical technologies may be implemented in farms where the lower operational costs do not compensate for the higher capital investment and process complexity of biological systems. The advantages and limitations of nitrogen removal and recovery technologies for wastewater streams have been recently reviewed by Beckinghausen et al. (2020), Campos et al. (2019) and Ye et al. (2018).

Struvite (magnesium ammonium phosphate, $MgNH_4PO_4 \cdot 6H_2O$) precipitation is a mature technology that is regaining interest due to its capacity to remove nutrients (nitrogen and/or phosphorous) while producing a slow-release fertiliser (Daneshgar et al., 2018; Kataki et al., 2016; Rahman et al., 2014). Struvite precipitation occurs when the product of magnesium (Mg^{2+}), phosphate (PO_4^{3-}) and ammonium ion (NH_4^+) concentrations exceeds struvite's solubility product (Daneshgar et al., 2019; Kazadi

Mbamba et al., 2015). Nonetheless, due to the equimolar composition of struvite, achieving high total ammoniacal nitrogen (TAN = NH_4^+ + NH_3) removal efficiency from pig slurry requires the addition of magnesium and phosphate since their concentration is very low compared to TAN concentration (El Diwani et al., 2007; Romero-Güiza et al., 2015b; Uludag-Demirer et al., 2005). The utilisation of commercial magnesium (e.g. $MgCl_2$, $Mg(OH)_2$, MgO) and phosphate (e.g. H_3PO_4, Na_2HPO_4, K_2HPO_4) reagents compromise the economic feasibility of struvite precipitation (Kataki et al., 2016; Wang et al., 2018; Ye et al., 2018). To overcome limitations associated with reagents cost, some researchers have explored the utilisation of low-cost magnesium sources, such as bittern (Etter et al., 2011; Lee et al., 2003), magnesite (Etter et al., 2011; Gunay et al., 2008), wood ash (Sakthivel et al., 2012; Xu et al., 2018) and low-grade magnesium oxide (LG-MgO) from the calcination of natural magnesite (Chimenos et al., 2003; Quintana et al., 2004; Romero-Güiza et al., 2015b; Al-Mallahi et al., 2020). The search for a phosphate-rich industrial wastewater or by-product remains an open quest by several research groups.

Santinelli et al. (2013) and Romero-Güiza et al. (2015b) using MgO as magnesium source observed that pre-mixing the MgO with phosphoric acid could lead to higher TAN removal efficiency than when the magnesium and the phosphate reagents were added separately. This feature represents an opportunity to further reduce struvite precipitation treatment cost. Romero-Güiza et al. (2014, 2015a, 2015b) named "stabilizing agent" (SA) the magnesium phosphate resulting from pre-mixing MgOs and phosphoric acid, which was described as a safe, easy to handle, non-invasive solid reagent. A further advantage of using the SA is the avoidance of NH_3 stripping and CO_2 effervescence associated with the direct dosage of MgO and H_3PO_4 in pig slurry, respectively. Importantly, Romero-Güiza et al. (2015b) noted that the efficiency of the SA was controlled by its composition,

with SAs formed by newberyite ($MgHPO_4 \cdot 3H_2O$) reaching higher TAN removal efficiency (~80%) than the stabilizing agents formed by bobierrite ($Mg_3(PO_4)_2 \cdot 8H_2O$) (~40%). These results were attributed to the higher solubility of newberyite in pig slurry (slightly alkaline medium) compared to bobierrite. Romero-Güiza et al. (2015b), who used four different MgOs, hypothesised that the less reactive MgOs favoured newberyite formation as a result of the lower pH during the synthesis, since newberyite formation is favoured at pH between 6.0 and 7.5 and bobierrite formation is favoured at alkaline pH (Bhuiyan, 2007; Tamimi et al., 2011). Besides pH, promoting newberyite formation requires more phosphate than bobierrite formation since newberyite has a higher P/Mg molar ratio than bobierrite (1.0 and 0.66, respectively). This knowledge opens a window of opportunity to optimise the formulation of stabilizing agents using low-grade MgO by developing formulation strategies that promote newberyite-rich SAs for cost-efficient struvite precipitation.

The goal of this study was to optimise the formulation of the stabilizing agent to synthesise a highly reactive stabilizing agent and improve the economic feasibility of struvite precipitation from pig slurry. To reach this goal, the first stages of this research focused on understanding the factors that control the nitrogen fixation efficiency of the stabilizing agent. The stabilizing agent was synthesised using LG-MgO as magnesium source and phosphoric acid as phosphate source. Formulation optimisation was carried out at lab-scale, while the optimum formulation was synthesised in a 200-L pilot-scale plant.

2. MATERIALS AND METHODS

2.1. Pig slurry and reagents

151 Two batches of pig slurry (liquid fraction after pig manure liquid-solid separation)
152 were collected from a breeder piggery farm located in Lleida (Spain). Pig slurry was
153 collected after the pig manure flushed from the housing floor was sieved through a 500
154 µm mesh. Pig slurry was stored in a refrigerated chamber at 4 ºC until use.

155 Reagent grade NH_4Cl (Panreac, S.A., Spain) was used to prepare the synthetic pig
156 slurry solution utilised to conduct the preliminary experiments (see Section 3.2). The
157 synthetic solution was prepared by diluting 3.9 grams of NH_4Cl per litre with deionized
158 water (ca. 1000 mg TAN/L solution) and adjusting the pH to ~7.0 with HCl. The impact
159 of the synthetic solution pH's on struvite precipitation results was tested by dosing a
160 carbonate-bicarbonate buffer solution to adjust the pH at 7.5 and at 8.5 (see Section 3.2).
161 The buffer solution was prepared diluting 7.69 g of $NaHCO_3$ and 0.95 g of Na_2CO_3 per
162 litre and subsequently adjusting the pH to 8.5 using a HCl concentrated solution.

163 The low-grade magnesium oxide (LG-MgO) used to formulate the stabilizing agent
164 was provided by Magnesistas Navarras, S.A. (Navarra, Spain). LG-MgO was collected
165 from the fabric filters of the air pollution control system of two rotatory kilns calcining
166 natural magnesite at 1100 ºC and at 1800 ºC to produce caustic calcined magnesia and
167 dead-burned magnesia, respectively. Table S1 and Fig. S1 in the supplementary material
168 show the semi-quantitative composition and X-ray diffractogram of the LG-MgO,
169 respectively. An 85% reagent-grade H_3PO_4 solution (VWR^{TM}, US) was used as phosphate
170 source to formulate the SA at lab-scale (ρ = 1.70 kg/L), while a 75% technical-grade
171 H_3PO_4 solution was used to formulate the SA in the 200-L pilot-scale plant (ρ = 1.58
172 kg/L).

173

174 *2.2. Stabilizing agent formulation*

175 The stabilizing agent (SA) was synthesised according to the procedure described in
176 Espiell et al. (2010) patent. First, a suspension of LG-MgO in deionised water (10% w/w)
177 was stirred for 15 min. Subsequently, the amount of phosphoric acid required to reach the
178 targeted H_3PO_4/LG-MgO ratio (in weight-basis) was added gradually in 3-4 steps to
179 control that the temperature was below 60 ºC. The suspension was stirred until the pH of
180 the solution remained stable (± 0.1) for 30 min. The total reaction time was about 4 hours.
181 Later, the SA particles were separated from the liquid by sedimentation (~2 hours) and
182 filtration (Büchner funnel) and subsequently dried in an oven at 105 °C until constant
183 weight. Finally, the solid filtered cake was disaggregated with a pestle and mortar. In the
184 pilot-scale plant, the final stages of the SA formulation process were adapted.
185 Specifically, the solid-liquid separation was done with a fabric membrane and the SA was
186 dried at room temperature for at least 2 days and mechanically disaggregated.
187 Several stabilizing agent formulations were synthesised during the course of this study
188 to assess (i) the impact of H_3PO_4/LG-MgO ratio on the stabilizing agent composition
189 (Section 3.1) and nitrogen removal efficiency (Section 3.2 and Section 3.3.1), (ii) the
190 reproducibility of the experimental results (Section 3.3.1), and (iii) the impact of the
191 H_3PO_4 solution grade used to formulate the SA (Section 3.3.4). The different SAs were
192 labelled according to the H_3PO_4/LG-MgO ratio used in their formulation. For instance, a
193 SA_0.85 means that 0.85 grams of H_3PO_4 were added per gram of LG-MgO.
194
195 *2.3. TAN removal experiments*
196 All TAN removal experiments were carried out in a jar test device (Velp Scientifica®
197 JT6) containing 0.5 L of synthetic solution or pig slurry. The experiments were done at
198 room temperature (18 - 22 °C) and under continuous stirring at 200 rpm. The dose of SA
199 added in all experiments was 12.5 g SA/g TAN, since this is the stoichiometric amount

of SA needed to completely remove all the TAN assuming that all the SA was only newberyite. In Section 3.3.3, the impact of different SA dose (8.5, 10.5, 12.5, 14.5 and 16.5 g SA/g TAN) on process efficiency was tested. All experiments were carried out in duplicate.

During the struvite precipitation experiments, TAN concentration and pH were measured at 0, 5, 10, 20, 30, 60, 120, 180 and 240 minutes. pH was measured with a portable pH-meter by soaking the probe in the reaction media and TAN was measured from 3 mL aliquots. For experiments using synthetic solution, the aliquot was directly filtered through a 0.45 μm regenerated cellulose syringe filter, while for experiments using pig slurry, the aliquot was centrifuged at 16000 × *g* for 5 min (Sigma 1-14 microcentrifuge) before filtered through a 0.45 μm regenerated cellulose syringe filter. The TAN removal efficiency of the SA was calculated by means of Equation (1), where TAN_0 is the initial TAN concentration (mg N/L) and TAN_t is the TAN concentration at a specific time.

$$\text{TAN removal efficiency}\ (\%) = \frac{TAN_0 - TAN_t}{TAN_0} \cdot 100 \qquad \text{Eq. 1}$$

The TAN removal capacity of the SA was calculated using Equation (2) and refers to the amount of TAN that a gram of SA can remove. In Eq. 2, SA_0 is the initial SA concentration (g SA/L).

$$\text{TAN removal capacity}\ (\text{g TAN/g SA}) = \frac{TAN_0 - TAN_t}{SA_0} \qquad \text{Eq. 2}$$

2.4. Analytical methods

pH was measured with a portable pH-meter (WTW^{TM} ProfiLine pH 3310) equipped with a universal pH electrode (WTW^{TM} SenTix$^{®}$). TAN was analysed following the Standard Methods procedure 4500-NH3D, using a Thermo Fisher Scientific ammonium ion-selective electrode (Orion 9512HPBNWP). Orthophosphate (PO_4^{3-}) was analysed using a Merck Spectroquant$^{®}$ test kit (range 1 – 100 mg P/L) and a spectrophotometer (Secoman UviLine 9100) following the protocol provided by the manufacturer.

The characterisation of the solid samples (i.e. LG-MgO, stabilizing agents and struvite precipitates) was carried out by X-ray fluorescence (XRF), X-ray diffraction (XRD) and scanning electron microscopy (SEM) combined with X-ray energy dispersive spectroscopy (EDS). Microscopy samples were carbon-coated. The major and minor elemental composition of the most stable oxides at 1100 ºC was determined by XRF using a Philips PW2400 X-ray sequential spectrophotometer. Crystalline mineral phases were identified by XRD using a Bragg–Brentano Siemens D-500 powder diffractometer device with CuK_{α} radiation. SEM micrographs were obtained with a SEM Quanta 200 FEI scanning electron microscope. EDS was used to obtain information about the elemental composition at different spots (about one cubic micron) of the solid particles. For SEM cross-section micrograph, samples were previously embedded in epoxy resin and then polished to show their inner morphology.

2.5. Economic analysis

The economic analysis of struvite precipitation using SA was performed considering that LG-MgO (branded as PC8) has a market price of 80 €/t and that the 75% H_3PO_4 solution has a market price of 580 €/t (i.e. 0.773 €/kg H_3PO_4). The amount of SA produced from each SA formulation and the TAN removal capacity of each SA was obtained from the lab-scale experiments (see values in Table S2). According to Section 3.3.3 results, it

was considered that the TAN removal capacity of the SAs was independent of the SA dose.

3. RESULTS AND DISCUSSION

3.1 Impact of H_3PO_4/LG-MgO ratio on the stabilizing agent properties

Fig. 1 shows the pH at the end of the SA synthesis carried out to analyse how different proportions between H_3PO_4 and LG-MgO affect (i) the pH of the reaction media, (ii) the characteristics of the resulting SA, and (iii) the SA's nitrogen removal efficiency (see Section 3.3).

The plot in Fig. 1 can be divided in 3 zones according to the pH pattern. In the first zone (from 0 to 0.3 g H_3PO_4/g LG-MgO), the pH decreased from 12.5 to 7.2 due to the neutralisation of $Ca(OH)_2$ and $Mg(OH)_2$ by H_3PO_4. In the second zone (between 0.3 and 1.05 g H_3PO_4/g LG-MgO), the pH remained stable at around 7.2, which was controlled by the solubility of the magnesium phosphate mineral phases (see Note S1 in the supplementary material). The presence of phosphate and carbonates in the solution may have also contributed to stabilise the pH around 7 (Valle-Zermeño et al., 2015). In the third zone (>1.05 g H_3PO_4/g LG-MgO), the pH decreased as the proportion of H_3PO_4 increased, which can be associated with an excess of H_3PO_4 in the reaction media.

XRF results showed that the P/Mg molar ratio of the SAs increased as the H_3PO_4/LG-MgO ratio increased (see Table S3 in the supplementary material). These results are consistent with the XRD results, which showed that the amount of newberyite in the SA increased to the detriment of bobierrite as the H_3PO_4/LG-MgO ratio increased (Fig. S2). Specifically, SA_0.65 and SA_0.72 were mostly formed by bobierrite, SA_0.78, SA_0.83 and SA_0.98 were formed by both bobierrite and newberyite (the bobierrite peak intensity in SA_0.98 was very weak), and SA_1.19 was the only

stabilizing agent where newberyite was the only determined magnesium phosphate (Table 1). These results indicate that, although the formation of bobierrite is favoured at alkaline pH and newberyite formation is favoured at slightly acidic pH, both bobierrite and newberyite can be obtained at neutral pH. At pH around 7.0, the H_3PO_4/LG-MgO ratio appears to be the factor controlling the magnesium phosphate resulting from the SA synthesis. It is worth noting that the solubility of the bobierrite at pH around 7.0 is much lower than the solubility of the newberyite (Romero-Güiza et al., 2015b).

SEM micrographs provided information on the stabilizing agents surface and cross-section structure and elemental composition (see Fig. S3 and Fig. S4). Magnification between 250x and 1000x showed that all the SA, except the SA_1.19, presented two types of particles: (1) crystal shaped and (2) round agglomerated shaped. The SA_1.19 was only formed by rounded particles, which were generally bigger than the particles obtained in other SAs. Observation at higher magnifications (up to 10000x) showed that the rounded particles in all SA were formed by the agglomeration of small crystals. The elemental composition of the crystal and rounded particles surface obtained by SEM-EDS showed that both particles were mainly composed of oxygen, magnesium and phosphorus, and small amounts of carbon and calcium. Thus, it appears that the shape and composition of the particles were not fully related. It is hypothesised that nucleation, crystal growth and particle size were controlled by the concentration of H_3PO_4 and the lower zeta-potential at higher H_3PO_4 doses. As the concentration of H_3PO_4 increased, the number of stable nuclei in the solution increased, and the crystal size decreased. However, the lower zeta-potential at higher H_3PO_4 doses favoured particles agglomeration by piercing and bonding which lead to bigger rounded particles. On the other hand, at lower H_3PO_4 concentrations, fewer stable nuclei were formed which lead in larger crystals

where the higher zeta potential prevented crystals agglomeration resulting in smaller particles.

Cross-section micrograph showed a white layer totally or partially surrounding the outskirt of several SA particles (Fig. S4). This white layer was associated with calcium phosphate precipitates since SEM-EDS showed that this layer had a remarkably high concentration of calcium when compared to other spots of the SA particles. Most particles also showed a different composition in their core, which was linked to unreacted periclase (MgO) due to the prevalence of magnesium and oxygen in the composition spectra. This observation confirms the hypothesis made in previous studies, where it was stated that the core of the LG-MgO did not react based on the shrinking core model (Romero-Güiza et al., 2015a, 2014).

The cross-section micrograph of the SA_1.19 was completely different to the other SA, since the cross-section of the particles were more homogeneous. Specifically, the core of the particles had a similar elemental composition to the rest of the particles, being oxygen, magnesium and phosphorus the main components. Small random irregularities in the SA_1.19 were related to the presence of calcium, iron and silicon. Overall, these results suggest that in the SA_1.19 formulation the reaction between H_3PO_4 and LG-MgO was nearly complete.

3.2 Stabilizing agent's nitrogen removal efficiency using synthetic solution

Fig. 2 shows that different SAs achieved different TAN removal efficiency with values ranging between 14% and 55%. The higher efficiencies were achieved by SAs containing both bobierrite and newberyite (i.e. SA_0.78 (55%), SA_0.83 (50%), SA_0.88 (36%)), whereas the SAs rich in newberyite showed much lower TAN removal efficiency (SA_0.98 (26%) and SA_1.19 (14%)). The efficiency of the two SAs only formed by

bobierrite was also low, 26% for both SA_0.65 and SA_0.72. These results were not in line with the experimental and modelling results of our previous study (Romero-Güiza et al., 2015b).

It was hypothesised that the different behaviour was related to the lack of alkalinity of the synthetic solution when compared to pig slurry. This may had prevented the pH increase from 6.5 to ~8.0 observed in our previous publications after 1 - 2 hours of experiment (Romero-Güiza et al., 2015a, 2015b). Indeed, struvite precipitation is well-known to be favoured at pH 8.0 - 9.5 (Battistoni et al., 2001; Doyle and Parsons, 2002; Kim et al., 2016). Accordingly, a TAN removal experiment was carried out where the pH of the reaction media was (i) not controlled, (ii) controlled at pH 7.5 after 100 min of experiment and (iii) controlled at pH 8.5 after 100 min of experiment (see Fig. S5). The pH of the solution was adjusted by adding dropwise a carbonate-bicarbonate buffer solution. For this experiment, a newberyite-rich SA was synthesised (i.e. SA_0.93). Experimental results showed that increasing the pH from 6.2 to 7.5 and 8.5 increased TAN removal from 38% to 47%. However, a 47% TAN removal efficiency was still lower than the values achieved in previous publications, where removal efficiencies above 60% were consistently achieved (Romero-Güiza et al., 2015b, 2014). Experimental results in Section 3.3, where pig slurry was used instead of a synthetic NH_4Cl solution, resulted in completely different results. These results showed that the matrix of the solution plays a crucial role in the SA behaviour (although the controlling factors remain unknown) and that using a synthetic NH_4Cl solution is not a valid experimental platform to simulate struvite precipitation from pig slurry.

3.3 Stabilizing agent's nitrogen removal efficiency using pig slurry

3.3.1 Yields and replicability

348 Fig. 3 shows the TAN removal efficiency of the two experiments carried out using pig
349 slurry. To guarantee the replicability of the results, each experiment was carried out using
350 a different pig slurry and SAs batch. Experimental results showed that (i) newberyite-rich
351 SA (i.e. SA_0.93, SA_0.98 and SA_1.09) achieved the highest TAN removal efficiency
352 with values ranging between 66% and 70%, which is in agreement with the TAN removal
353 efficiency obtained in previous studies (Romero-Güiza et al., 2015b, 2014), and (ii) the
354 TAN removal efficiency decreased as the H_3PO_4/LG-MgO ratio used to synthesise the
355 SA decreased. The latter is consistent with the higher abundance of bobierrite in the SAs
356 synthesised at H_3PO_4/LG-MgO ratios below 0.98 (Table 1). These results also showed
357 that the experiments were replicable since the yield achieved in both experiments was
358 remarkably similar considering that they were done using two independent pig slurry and
359 SAs batches.
360 The TAN removal capacity of the SA_0.93, SA_0.98 and SA_1.09 was 0.055
361 g TAN/g SA, representing 70% of the maximum efficiency if all the SA was newberyite
362 (max. 0.080 g TAN/g SA). However, both XRF and XRD clearly showed that besides
363 MgO, the LG-MgO contained brucite, calcite, dolomite, magnesite, lime and quartz
364 among others (see Table S1 and Fig. S1). Indeed, assuming that all the MgO was
365 converted to newberyite, it was estimated that MgO represented about 58% of the LG-
366 MgO total weight. This figure is expected to be a bit higher due to the presence of MgO
367 in the core of the SA particles and unreacted magnesium phosphates.

368 *3.3.2 Impact of SA's particle size*

369 Reducing the particle size by grinding the SA_0.93, SA_0.98 and SA_1.09 in an
370 agatha disc mill (Retsch RS 100) at 700 rpm for 15 minutes did not improve the TAN
371 removal efficiency of the SAs (Fig. S6). These results indicated that the TAN removal
372 efficiency was not controlled by the SA particles surface area either because (i) the

particle size of the SA was not largely affected by the grinding process (most particles had a particle size <200 μm) or, as suggested in Romero-Güiza et al. (2015b), because newberyite-rich SAs completely dissolves in the pig slurry to effectively precipitate struvite.

3.3.3 Impact of SA dose

The TAN removal capacity obtained in the previous experiments for SA_0.93, SA_0.98 and SA_1.09 was consistently 0.055 g TAN/g SA (Section 3.3.1 and 3.3.2). However, these experiments were obtained using the same SA dose, i.e. 12.5 grams of SA per gram of TAN (equal to the amount of SA needed to completely remove all the TAN if the SA was entirely newberyite). However, different SA doses will be needed depending on the percentage of TAN to be removed. From a technical and economic point of view, it is important to know whether the TAN removal capacity of the SA is proportional to the dose. Therefore, an experiment was carried out using five doses, i.e. 8.5, 10.5, 12.5, 14.5 and 16.5 g SA/g TAN. In this experiment, the SA_0.98 was used.

Experimental results showed that the higher the SA dose, the higher the TAN removal (Fig. S7). The highest SA dose (i.e. 16.5 g SA/g TAN) was able to remove 80% of the TAN, which decreased the pig slurry TAN concentration from 2.5 to 0.5 g TAN/L. The 12.5 g SA/g TAN removed 67% of the TAN, which was in agreement with all previous experiments. The removal capacity of the 10.5, 12.5, 14.5 and 16.5 g SA/g TAN doses was 0.048 - 0.054 g TAN/g SA ($P > 0.113$). However, the 8.5 g SA/g TAN dose showed a significantly lower TAN removal capacity of 0.044 g TAN/g SA ($P = 0.027$ when compared to 12.5 g SA/g TAN). The 18% lower TAN removal capacity of the 8.5 g SA/g TAN dose implies that higher doses of SA will be needed when targeting TAN removal efficiency below 50%. This loss of capacity could be explained by the rapid

398 formation of a struvite coating layer on the SA particle, which may have limited
399 newberyite dissolution.
400
401 *3.3.4 Comparison between lab-scale and pilot-scale SA synthesis*
402 The TAN removal efficiency of the SA_0.98 synthesised in the pilot-scale plant using
403 the same LG-MgO and a 75% technical-grade H_3PO_4 solution was tested and compared
404 with two SA_0.98 synthesised in the lab. The difference between the two SAs synthesised
405 in the lab was the phosphoric acid source since one used the 75% H_3PO_4 solution used in
406 the pilot-pant, and the other used the 85% reagent-grade H_3PO_4 solution used in all
407 previous SA synthesis. XRD results showed that newberyite was the dominant
408 magnesium phosphate of the three SAs, although bobierrite was detected in the SA
409 synthesised in the pilot-plant (Fig. S9).
410 Experimental results showed that H_3PO_4 solution does not have a significant impact
411 on the SA's TAN removal capacity ($P = 0.614$) since the two SA synthesised in the lab
412 averaged a TAN removal capacity of 0.057 g TAN/g SA (Fig. S8). However, the SA
413 synthesised in the pilot-plant showed a slightly lower TAN removal capacity of 0.052 g
414 TAN/g SA ($P < 0.05$), which is consistent with the presence of bobierrite in the SA. These
415 differences can be attributed to geometric differences of the SA synthesis tank as well as
416 the effectiveness of stirring and temperature during the SA synthesis. However, a 10%
417 difference between the SA synthesised at lab-scale and pilot-scale is within the expected
418 loss of effectiveness when scaling-up a chemical process. Finally, it is worth mentioning
419 that XRD patterns of the precipitates confirmed that struvite was formed during the TAN
420 removal experiments (Fig. S10). The XRD patterns of the precipitates also showed that
421 the solid still had some unreacted newberyite, which could be attributed to the formation
422 of a struvite coating layer on the SA particle, but also due to the limited reaction time (4

hours). It should be noted that preliminary experiments lasting 24 hours showed that SA removed >95% of TAN during the first 4 hours (data not shown).

3.4 Economic analysis of using SA to remove nitrogen from pig slurry

The cost of the SA is dictated by the phosphoric acid price since it is ten times more expensive than the LG-MgO. However, the low reactivity of LG-MgO is key to promote the formation of newberyite (Romero-Güiza et al., 2015b) and make an efficient use of the phosphoric acid. Specifically, the SA's reagents cost increased from 0.38 €/kg_{SA} (SA_0.78) to 0.42 €/kg_{SA} (SA_1.09) as the H_3PO_4/LG-MgO ratio increased. The amount of SA produced per kg of LG-MgO also increased with the H_3PO_4/LG-MgO ratio, which was expected considering that more phosphate reacted with the LG-MgO. For H_3PO_4/LG-MgO ≤1.09, the phosphate concentration in the reaction liquor at the end of the synthesis was always below 100 mg P/L.

The cost of the SA increased as the H_3PO_4/LG-MgO increased, however, the noticeable gain in reactivity (i.e. TAN removal capacity) compensates the higher cost. Specifically, the cost to remove 1 kg of TAN decreased from 8.8 € (SA_0.78) to 7.5 € (SA_0.98) (see Table S2). Although SA_1.09 was the most reactive SA, SA_0.98 was the formulation that showed the cheapest treatment cost since the slightly higher reactivity of SA_1.09 did not compensate for the higher H_3PO_4 consumption. Using the SA_0.98, the cost to remove 50% of the TAN from fresh pig slurry with a 1500, 2000 and 2500 mg TAN/L is estimated at 5.6, 7.5 and 9.4 €/m^3, respectively. This economic analysis did not consider other operational costs (e.g. pumping, mixing, reagents), capital costs and potential revenues from struvite commercialisation. Importantly, experimental results showed that the spent reaction liquor (water with ~100 mg P/L) can be reused multiples times without affecting the SA reactivity (data not shown). This is important since it

minimises water usage and avoids the need for wastewater treatment. Finally, as shown in Section 3.1, it is worth highlighting that the wastewater matrix may influence the TAN removal capacity of the SA.

CONCLUSIONS

This study aimed to optimise the formulation of a stabilizing agent (SA) for efficient TAN recovery from pig slurry via struvite precipitation. The SA was synthesised using a low-grade MgO by-product (LG-MgO) and phosphoric acid. Experimental results showed that the H_3PO_4/LG-MgO ratio controls the magnesium phosphate mineral phase (bobierrite and/or newberyite) of the SA, with H_3PO_4/LG-MgO ratio ≥0.98 leading to SAs mainly formed of newberyite. Synthesising a newberyite-rich SA is important since it allowed achieving higher TAN removal efficiency from pig manure (66 – 73%) than the SA formed by a mixture of newberyite and bobierrite (51 – 59%) and by bobierrite (<30%) (dose of 12.5 g SA/g TAN). XRD patterns showed that the precipitates contained some unreacted newberyite, however, particle size reduction did not improve the TAN removal efficiency of the SAs. The economic analysis showed that gain in reactivity of the SA synthesised with higher H_3PO_4/LG-MgO ratios compensated the higher SA reagent cost, where SA_0.98 (H_3PO_4/LG-MgO ratio of 0.98) showed the lowest treatment cost. The cost to remove 1 kg of ammonia nitrogen from fresh pig slurry using the SA_0.98 was estimated at 7.5 €. Finally, the SA_0.98 was successfully synthesised in a 200-L pilot plant, which SA only showed a 10% lower TAN removal capacity (0.052 g TAN/g SA) than the one synthesised in the lab (0.057 g TAN/g SA).

ACKNOWLEDGEMENTS

This research was funded by the Rural Development Program of the Government of Catalonia, GO. 16.01.01 (file number 5621 002 2016 P4) supported by the European Agricultural Fund for Rural Development (FEADER). The authors also thank the Spanish Ministry of Science and Innovation (RTC2019-007257-5) for their funding support. Sergi Astals is grateful to the Spanish Ministry of Science, Innovation and Universities for his Ramon y Cajal fellowship (RYC-2017-22372). Sergio Huete-Hernández is grateful to the Government of Catalonia and the University of Barcelona for the Research Grant (APIF-DGR 2018). The authors are thankful to MSc. Eduard Marot for his excellent technical assistance in the lab and Mr. David Terreros (Gasporc, S.A.) for setting-up and conducting the SA synthesis in the pilot-scale plant. The authors are grateful to SAT La Vall Soses and Magnesitas Navarras, S.A. for providing pig slurry and LG-MgO samples, respectively.

REFERENCES

Al-Mallahi, J., Sürmeli, R.Ö., Çalli, B., 2020. Recovery of phosphorus from liquid digestate using waste magnesite dust. Journal of Cleaner Production 272, 122616. https://doi.org/10.1016/j.jclepro.2020.122616

Bationo, A., Kihara, J., Vanlauwe, B., Waswa, B., Kimetu, J., 2007. Soil organic carbon dynamics, functions and management in West African agro-ecosystems. Agricultural Systems, Making Carbon Sequestration Work for Africa's Rural Poor 94, 13–25. https://doi.org/10.1016/j.agsy.2005.08.011

Battistoni, P., De Angelis, A., Pavan, P., Prisciandaro, M., Cecchi, F., 2001. Phosphorus removal from a real anaerobic supernatant by struvite crystallization. Water Research 35, 2167–2178. https://doi.org/10.1016/S0043-1354(00)00498-X

Beckinghausen, A., Odlare, M., Thorin, E., Schwede, S., 2020. From removal to recovery: An evaluation of nitrogen recovery techniques from wastewater. Applied Energy 263, 114616. https://doi.org/10.1016/j.apenergy.2020.114616

Bhuiyan, Md.I.H., 2007. Investigation into struvite solubility, growth and dissolution kinetics in the context of phosphorus recovery from wastewater (PhD Thesis). Retrospective Theses and Dissertations, 1919-2007. University of British Columbia. https://doi.org/10.14288/1.0063242

Campos, J.L., Crutchik, D., Franchi, Ó., Pavissich, J.P., Belmonte, M., Pedrouso, A., Mosquera-Corral, A., Val del Río, Á., 2019. Nitrogen and Phosphorus Recovery From Anaerobically Pretreated Agro-Food Wastes: A Review. Front. Sustain. Food Syst. 2. https://doi.org/10.3389/fsufs.2018.00091

Chimenos, J.M., Fernández, A.I., Villalba, G., Segarra, M., Urruticoechea, A., Artaza, B., Espiell, F., 2003. Removal of ammonium and phosphates from wastewater resulting

509 from the process of cochineal extraction using MgO-containing by-product. Water
510 Research 37, 1601–1607. https://doi.org/10.1016/S0043-1354(02)00526-2
511 Cruz, H., Law, Y.Y., Guest, J.S., Rabaey, K., Batstone, D., Laycock, B., Verstraete, W., Pikaar,
512 I., 2019. Mainstream Ammonium Recovery to Advance Sustainable Urban Wastewater
513 Management. Environ. Sci. Technol. 53, 11066–11079.
514 https://doi.org/10.1021/acs.est.9b00603
515 Daneshgar, S., Callegari, A., Capodaglio, A.G., Vaccari, D., 2018. The Potential Phosphorus
516 Crisis: Resource Conservation and Possible Escape Technologies: A Review. Resources
517 7, 37. https://doi.org/10.3390/resources7020037
518 Daneshgar, S., Vanrolleghem, P.A., Vaneeckhaute, C., Buttafava, A., Capodaglio, A.G., 2019.
519 Optimization of P compounds recovery from aerobic sludge by chemical modeling and
520 response surface methodology combination. Science of The Total Environment 668,
521 668–677. https://doi.org/10.1016/j.scitotenv.2019.03.055
522 De Vrieze, J., Colica, G., Pintucci, C., Sarli, J., Pedizzi, C., Willeghems, G., Bral, A., Varga, S.,
523 Prat, D., Peng, L., Spiller, M., Buysse, J., Colsen, J., Benito, O., Carballa, M.,
524 Vlaeminck, S.E., 2019. Resource recovery from pig manure via an integrated approach:
525 A technical and economic assessment for full-scale applications. Bioresource
526 Technology 272, 582–593. https://doi.org/10.1016/j.biortech.2018.10.024
527 Doyle, J.D., Parsons, S.A., 2002. Struvite formation, control and recovery. Water Research 36,
528 3925–3940. https://doi.org/10.1016/S0043-1354(02)00126-4
529 El Diwani, G., El Rafie, Sh., El Ibiari, N.N., El-Aila, H.I., 2007. Recovery of ammonia nitrogen
530 from industrial wastewater treatment as struvite slow releasing fertilizer. Desalination
531 214, 200–214. https://doi.org/10.1016/j.desal.2006.08.019
532 Espiell, F., Segarra, M., Chimenos, J.M., Fernández, A.I., 2010. Method for reducing the
533 concentration of ammonium in excrement on cattle farms. WO2010018260A1.
534 Etter, B., Tilley, E., Khadka, R., Udert, K.M., 2011. Low-cost struvite production using source-
535 separated urine in Nepal. Water Research 45, 852–862.
536 https://doi.org/10.1016/j.watres.2010.10.007
537 García-González, M.C., Riaño, B., Teresa, M., Herrero, E., Ward, A.J., Provolo, G., Moscatelli,
538 G., Piccinini, S., Bonmatí, A., Bernal, M.P., Wiśniewska, H., Proniewicz, M., García-
539 González, M.C., Riaño, B., Teresa, M., Herrero, E., Ward, A.J., Provolo, G., Moscatelli,
540 G., Piccinini, S., Bonmatí, A., Bernal, M.P., Wiśniewska, H., Proniewicz, M., 2016.
541 Treatment of swine manure: case studies in European's N-surplus areas. Scientia
542 Agricola 73, 444–454. https://doi.org/10.1590/0103-9016-2015-0057
543 Giner Santonja, G., Konstantinos, G., Maria, S.B., Paolo, M., Serge, R., Delgado Sancho, L.,
544 2017. Best Available Techniques (BAT) Reference Document for the Intensive Rearing
545 of Poultry or Pigs. Industrial Emissions Directive 2010/75/EU (Integrated Pollution
546 Prevention and Control).
547 Gunay, A., Karadag, D., Tosun, I., Ozturk, M., 2008. Use of magnesit as a magnesium source
548 for ammonium removal from leachate. Journal of Hazardous Materials 156, 619–623.
549 https://doi.org/10.1016/j.jhazmat.2007.12.067
550 Kamilaris, A., Engelbrecht, A., Pitsillides, A., Prenafeta-Boldú, F.X., 2020. Transfer of manure
551 as fertilizer from livestock farms to crop fields: The case of Catalonia. Computers and
552 Electronics in Agriculture 175, 105550. https://doi.org/10.1016/j.compag.2020.105550
553 Kataki, S., West, H., Clarke, M., Baruah, D.C., 2016. Phosphorus recovery as struvite: Recent
554 concerns for use of seed, alternative Mg source, nitrogen conservation and fertilizer
555 potential. Resources, Conservation and Recycling 107, 142–156.
556 https://doi.org/10.1016/j.resconrec.2015.12.009
557 Kazadi Mbamba, C., Tait, S., Flores-Alsina, X., Batstone, D.J., 2015. A systematic study of
558 multiple minerals precipitation modelling in wastewater treatment. Water Research 85,
559 359–370. https://doi.org/10.1016/j.watres.2015.08.041
560 Kim, D., Min, K.J., Lee, K., Yu, M.S., Park, K.Y., 2016. Effects of pH, molar ratios and pre-
561 treatment on phosphorus recovery through struvite crystallization from effluent of
562 anaerobically digested swine wastewater. Environmental Engineering Research 22, 12–
563 18. https://doi.org/10.4491/eer.2016.037

564 Lee, S.I., Weon, S.Y., Lee, C.W., Koopman, B., 2003. Removal of nitrogen and phosphate from
565 wastewater by addition of bittern. Chemosphere 51, 265–271.
566 https://doi.org/10.1016/S0045-6535(02)00807-X
567 Musacchio, A., Re, V., Mas-Pla, J., Sacchi, E., 2020. EU Nitrates Directive, from theory to
568 practice: Environmental effectiveness and influence of regional governance on its
569 performance. Ambio 49, 504–516. https://doi.org/10.1007/s13280-019-01197-8
570 Quintana, M., Colmenarejo, M.F., Barrera, J., García, G., García, E., Bustos, A., 2004. Use of a
571 byproduct of magnesium oxide production to precipitate phosphorus and nitrogen as
572 struvite from wastewater treatment liquors. J. Agric. Food Chem. 52, 294–299.
573 https://doi.org/10.1021/jf0303870
574 Rahman, Md.M., Salleh, M.A.Mohd., Rashid, U., Ahsan, A., Hossain, M.M., Ra, C.S., 2014.
575 Production of slow release crystal fertilizer from wastewaters through struvite
576 crystallization – A review. Arabian Journal of Chemistry, Special Issue: Environmental
577 Chemistry 7, 139–155. https://doi.org/10.1016/j.arabjc.2013.10.007
578 Report SWD(2018)246 final, 2108. Report from the commission to the council and the
579 European Parliamnet on the implementation of Council Directive 91/676/EEC
580 concerning the protection of waters against pollution caused by nitrates from
581 agricultural sources based on Member State reports for the period 2012–2015.
582 Romero-Güiza, M.S., Astals, S., Chimenos, J.M., Martínez, M., Mata-Alvarez, J., 2014.
583 Improving anaerobic digestion of pig manure by adding in the same reactor a stabilizing
584 agent formulated with low-grade magnesium oxide. Biomass and Bioenergy 67, 243–
585 251. https://doi.org/10.1016/j.biombioe.2014.04.034
586 Romero-Güiza, M.S., Astals, S., Mata-Alvarez, J., Chimenos, J.M., 2015a. Feasibility of
587 coupling anaerobic digestion and struvite precipitation in the same reactor: Evaluation
588 of different magnesium sources. Chemical Engineering Journal 270, 542–548.
589 https://doi.org/10.1016/j.cej.2015.02.057
590 Romero-Güiza, M.S., Tait, S., Astals, S., del Valle-Zermeño, R., Martínez, M., Mata-Alvarez,
591 J., Chimenos, J.M., 2015b. Reagent use efficiency with removal of nitrogen from pig
592 slurry via struvite: A study on magnesium oxide and related by-products. Water
593 Research 84, 286–294. https://doi.org/10.1016/j.watres.2015.07.043
594 Sakthivel, S.R., Tilley, E., Udert, K.M., 2012. Wood ash as a magnesium source for phosphorus
595 recovery from source-separated urine. Science of The Total Environment 419, 68–75.
596 https://doi.org/10.1016/j.scitotenv.2011.12.065
597 Santinelli, M., Eusebi, A.L., Santini, M., Battistoni, P., 2013. Struvite Crystallization for
598 Anaerobic Digested Supernatants: Influence on the Ammonia Efficiency of the Process
599 Variables and the Chemicals Dosage Modality. Icheap-11: 11th International
600 Conference on Chemical and Process Engineering, Pts 1-4 32, 2047–2052.
601 https://doi.org/10.3303/cet1332342
602 Siegrist, H., 1996. Nitrogen removal from digester supernatant-comparison of chemical and
603 biological methods. Water science and Technology 34, 399–406.
604 Sommer, S.G., Clough, T.J., Balaine, N., Hafner, S.D., Cameron, K.C., 2017. Transformation of
605 Organic Matter and the Emissions of Methane and Ammonia during Storage of Liquid
606 Manure as Affected by Acidification. Journal of Environmental Quality 46, 514–521.
607 https://doi.org/10.2134/jeq2016.10.0409
608 Tamimi, F., Nihouannen, D.L., Bassett, D.C., Ibasco, S., Gbureck, U., Knowles, J., Wright, A.,
609 Flynn, A., Komarova, S.V., Barralet, J.E., 2011. Biocompatibility of magnesium
610 phosphate minerals and their stability under physiological conditions. Acta
611 Biomaterialia 7, 2678–2685. https://doi.org/10.1016/j.actbio.2011.02.007
612 Türker, M., Çelen, I., 2007. Removal of ammonia as struvite from anaerobic digester effluents
613 and recycling of magnesium and phosphate. Bioresource Technology 98, 1529–1534.
614 https://doi.org/10.1016/j.biortech.2006.06.026
615 Uludag-Demirer, S., Demirer, G.N., Chen, S., 2005. Ammonia removal from anaerobically
616 digested dairy manure by struvite precipitation. Process Biochemistry 40, 3667–3674.
617 https://doi.org/10.1016/j.procbio.2005.02.028

618 Valle-Zermeño, R., Giro-Paloma, J., Formosa, J., Chimenos, J.M., 2015. Low-grade magnesium
619 oxide by-products for environmental solutions: Characterization and geochemical
620 performance. Journal of Geochemical Exploration 152, 134–144.
621 https://doi.org/10.1016/j.gexplo.2015.02.007
622 Wang, J., Ye, X., Zhang, Z., Ye, Z.-L., Chen, S., 2018. Selection of cost-effective magnesium
623 sources for fluidized struvite crystallization. Journal of Environmental Sciences 70,
624 144–153. https://doi.org/10.1016/j.jes.2017.11.029
625 Xu, K., Lin, F., Dou, X., Zheng, M., Tan, W., Wang, C., 2018. Recovery of ammonium and
626 phosphate from urine as value-added fertilizer using wood waste biochar loaded with
627 magnesium oxides. Journal of Cleaner Production 187, 205–214.
628 https://doi.org/10.1016/j.jclepro.2018.03.206
629 Ye, Y., Ngo, H.H., Guo, W., Liu, Y., Chang, S.W., Nguyen, D.D., Liang, H., Wang, J., 2018. A
630 critical review on ammonium recovery from wastewater for sustainable wastewater
631 management. Bioresource Technology 268, 749–758.
632 https://doi.org/10.1016/j.biortech.2018.07.111
633

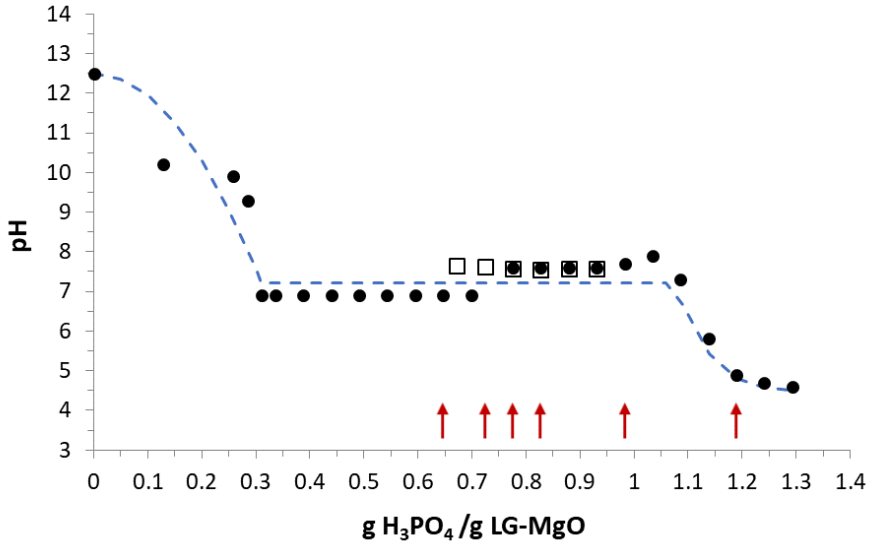

Fig. 1. Final pH of the stabilizing agent synthesis carried out at different H_3PO_4/LG-MgO ratios. (●) identifies results from the first synthesis, (□) identifies results from second synthesis done to confirm the results, (↑) point out to the samples analysed by XRF, XRD and SEM. Dashed blue line indicates the pH pattern.

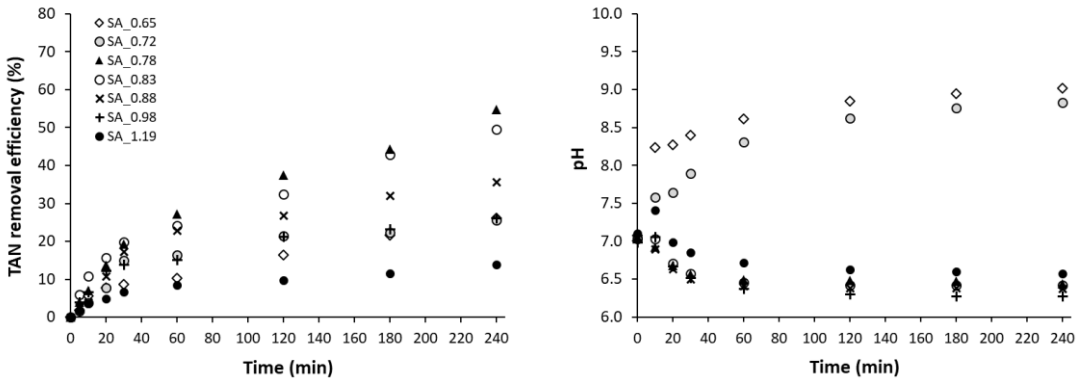

Fig. 2. Results from the TAN removal experiments carried out with the synthetic solution without buffer (TAN_0 = 1130 mg TAN/L). (left) TAN removal efficiency and (right) pH over time.

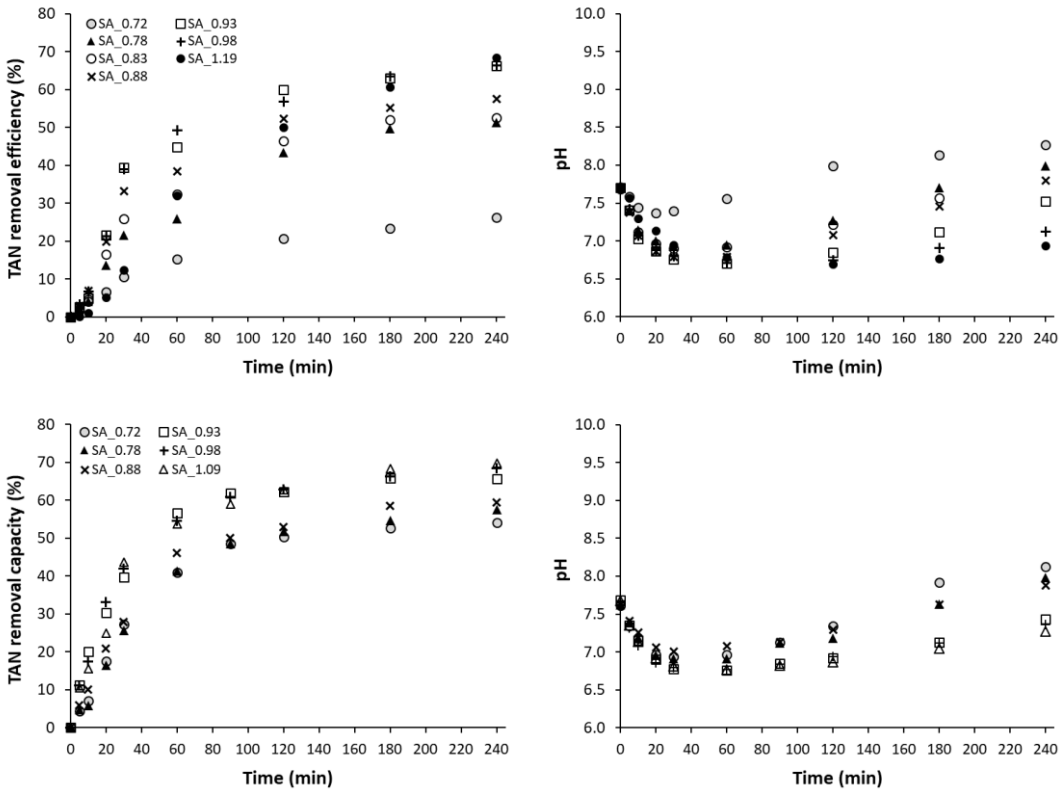

Fig. 3. TAN removal efficiency and pH values over time for the TAN removal experiments carried out with pig slurry. (top) batch 1 (TAN_0 = 2010 mg TAN/L), (bottom) batch 2 (TAN_0 = 1495 mg TAN/L).